Proceedings 10th NUMGE 2023
10th European Conference on Numerical Methods in Geotechnical Engineering
Zdravkovic L, Kontoe S, Taborda DMG, Tsiampousi A (eds)

https://doi.org/10.53243/NUMGE2023-330

Three-dimensional finite element modelling to assess the damage due to boulder impact during pile installation

F. Palmieri[1], D. McLennan[1], F. Ciruela-Ochoa[1], A. Cunningham[1], J. Go[1], P. Morrison[1], C. Tejada[2], G. Perikleous[3], J. Brandt[3], M. Lubek[4]

[1]*Ove Arup & Partners, London, UK*
[2]*Ørsted A/S, London, UK*
[3]*Ørsted A/S, Copenhagen, DK*
[4]*Ørsted A/S, Skærbæk, DK*

ABSTRACT: Pile damage due to impact with a boulder during driving is a major risk during offshore wind foundation installation. A numerical assessment of this damage accounting for the pile-boulder-soil interaction is presented in this paper. Three-dimensional (3D) dynamic finite-element (FE) analyses were carried out with LS-DYNA FE program for simulating the monopile (MP) driving process. Boulder impact was simulated by: 1) using a hammer assembly to impart a single impact onto MP and boulder, and 2) pushing the MP at a constant velocity towards the boulder. Various soil properties and boulder dimensions were considered. The steel MP was modelled using thick shell elements with elasto-plastic behaviour. The boulder was modelled as an elastic sphere with solid elements. The resistance of the soil surrounding boulder and MP was modelled with non-linear springs. These non-linear springs were calibrated using 3D FE analyses simulating the soil displacement due to boulder push and MP driving. The 3D model without boulder was validated against results from GRLWEAP software, applying one-dimensional stress wave propagation theory for drivability assessment. This study was used to influence on-site MP driving strategy to minimise the risk of MP damage and refusal.

Keywords: Finite element; Offshore; Foundation, Damage, Boulder

1 INTRODUCTION

Monopiles (MP) are commonly used as foundations for offshore wind turbines and are typically top driven into the seafloor using hydraulic impact hammers. For sites with a history of glaciation, the presence of boulders can pose a significant challenge to MP installation as boulders can make it difficult to drive MPs to the required depth and can increase the risk of MP damage during installation. Three-dimensional finite element analysis (3D FEA) is an important tool for assessing MP damage during pile driving, as it allows for detailed modelling and simulation of the dynamic loading conditions and material behaviour. This paper shows how 3D FEA can provide insight into the extent and location of MP damage due to extrusion buckling and can increase the safety and reliability of the MP.

2 NUMERICAL STUDY

2.1 Overview

The structural performance of a MP impacting a boulder was evaluated using FEA. The numerical assessment of the MP-boulder-soil interaction was conducted in LS-DYNA (Hallquist, 2006), an explicit finite element (FE) code enabling the computation of highly non-linear three-dimensional problems.

The study considered the presence of the boulder in two scenarios: *i)* an initial impact with the boulder following an explicitly modelled hammer blow; *ii)* the subsequent push of the boulder leading to localised MP distortion and distortional buckling during the remaining drive. For the first scenario, the model considered a hammer assembly imparting a single blow onto the MP and boulder (Section 0). For the second scenario, the model excluded the hammer assembly and considered the MP impacting and moving past the boulder at a constant velocity (Section 2.5). In both cases, the soil surrounding the MP and boulder was modelled with non-linear spring elements and associated dampers to allow more sensitivity studies and to avoid long run-times (Nietiedt et al, 2022) which are not suitable in practice. Properties for the non-linear springs and dampers were calibrated to match the ground model (Section 2.3).

2.2 MP-boulder-soil model

The boulder impact was simulated using the FE model shown in Figure 1. As described in the previous section,

depending on the specific scenario, the model includes the following components:

1. the MP,
2. the hammer assembly (anvil and hammer) with a specified initial kinetic energy,
3. non-linear springs and dampers to represent the soil resistance onto the lateral surface of the MP in the radial and vertical directions. These elements were set-up to activate at their contact with the MP during its driving into the seabed, so that at any penetration depth, only the embedded part of the MP was surrounded by active elements,
4. non-linear springs and dampers to represent the soil resistance at the toe of the MP in the vertical direction. These elements were set-up to update their properties during driving to capture the variation of the soil properties with depth.
5. an idealised spherical boulder,
6. non-linear springs and dampers to represent the translational (horizontal and vertical) and rotational soil resistance around the boulder.

The MP was modelled using thick shell elements with elasto-plastic material properties and strain-rate enhancement using Cowper-Symonds based upon DNV-RP-C208 (2016). The boulder was modelled using solid elements with elastic material properties, thus, its breakage was conservatively excluded from the study.

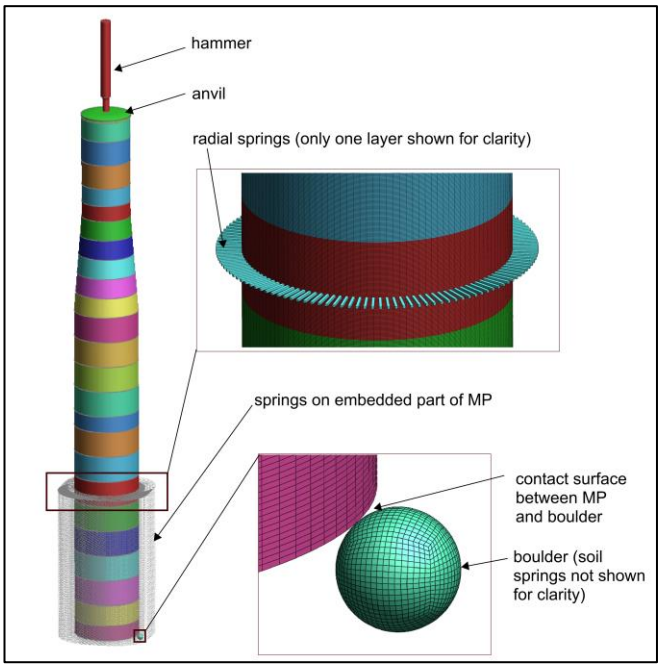

Figure 1. Finite element model for boulder impact analysis

2.3 Derivation of soil resistance properties

A representative soil profile and associated parameters were determined based on the available in-situ and laboratory tests. A series of sampling borheoles as well as cone penetration tests (CPTs) measuring pore water pressures and small-strain soil parameters were executed. Laboratory tests included moisture content, Atterberg limits, maximum and minimum dry density, and particle size distribution. The deposit used for this paper primarly consisted of an overconsolidated clay. To this deposit, lower and upper bound (LB and UB) soil properties were assigned to account for the uncertainties during the ground characterization stage. On average, the LB values of the small strain stiffness and undrained shear strength were assessed as 20% and 35% of the corresponding UB value, respectively. As discussed in Section 2.2, the modelling approach considered the soil by means of non-linear springs. These springs were characterized based upon force-displacement curves representing the soil response to the MP and boulder movements.

Toe resistance and skin friction were derived following the approach by Alm and Hamre (2001). This approach is based on CPT data and accounts for the friction fatigue due to driving by the reduction of the side friction. The size and location of the boulder considered in the study is based on a probabilistic boulder assessment. The boulder's translational resistance was characterized based on the results of 3D FEA simulating the soil-boulder interaction due to the impact with the MP. The adopted soil constitutive model accounted for the non-linearity characterizing the small-strain behaviour. Hysteretic properties were characterized based on Darendeli (2001) accounting for the effects of effective stress, soil plasticity and OCR. These poperties were further modified to allow the prediction of the undrained shear strength at an assumed shear strain at failure of 10% following the procedure outlined in Yin et al. (2013). The adopted boulder-soil model considers half of the soil domain surrounding the boulder at a specified depth (see Figure 2). In this model, boundary conditions at the bottom are fixed while the edges are roller supported to allow the vertical displacement. It was assumed that the boulder could be displaced either radially or vertically away as the MP impacts the boulder. Thus, a vertical and horizontal displacement were applied to the boulder to derive the surrounding soil response. An example of the resultant displacement vectors developing within the soil due to a horizontal push of the boulder and corresponding force-displacement curve are shown in Figure 2. The rotational resistance of the soil surrounding the boulder was hand-calculated based on the soil undrained shear strength.

Finally, the radial resistance was also characterized based on 3D FEA simulating the cylindrical cavity expansion due to MP installation whereby radial displacements are prescribed to the edge of the cavity. Figure 3

shows an isometric view of the adopted model consisting of a 15° sector of a cylindrical soil domain with a mesh refinement near the edge of the cavity. In this model, boundary conditions allow the soil to move radially from the edge of the cavity outwards. From this analysis, pressure-displacement curves at various depths were derived for the MP radial springs. These curves act in tension and compression depending on if the MP is moving inward or outward.

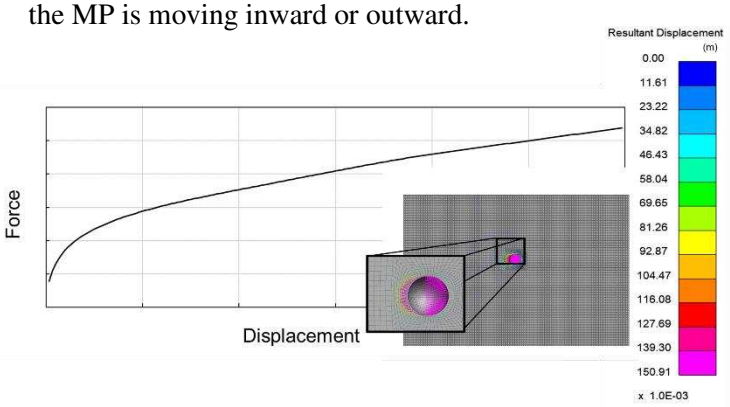

Figure 2. Example of horizontal force-displacement curve adopted for the calibration of the translational boulder resistance and 3D FE model for its evaluation

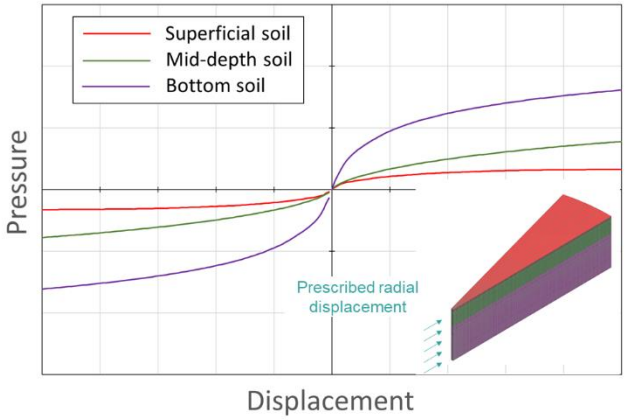

Figure 3. Example of pressure-displacement curves adopted for the calibration of the MP radial resistance and 3D FE model for their evaluation

2.4 Hammer impact analysis

The aim of this analysis was to predict the behaviour of the MP hitting a boulder under the loading induced by a hammer impact as shown in Figure 4. This includes the stress waves propagating from the hammer impact, the inertial effect of the boulder, as well as the soil resistance. An example of the waves propagating down the height of the MP can be seen in Figure 4. The ripples are caused by several factors including changes in the thickness and diameter of the MP. The hammer assembly was modelled with respect to its specifications given as input (e.g., MENCK MHU4400S) and by ensuring that the correct impact energy was applied during the analysis.

Simulations with no boulder were initially conducted to compare the FE model predictions against the results obtained with the established GRLWEAP (Pile Dynamics, Inc.) software (Goble and Rausche, 1976). GRLWEAP is a one-dimensional Wave Equation Analysis program that models the MP driving process. The GRLWEAP inputs include the MP geometry, soil parameters and type of hammer which were specified consistently to the FE model. The evolution of the toe displacement with time as predicted by LS-DYNA and GRLWEAP in the absence of boulder is shown in Figure 5. A reasonable agreement between the two predictions can be observed.

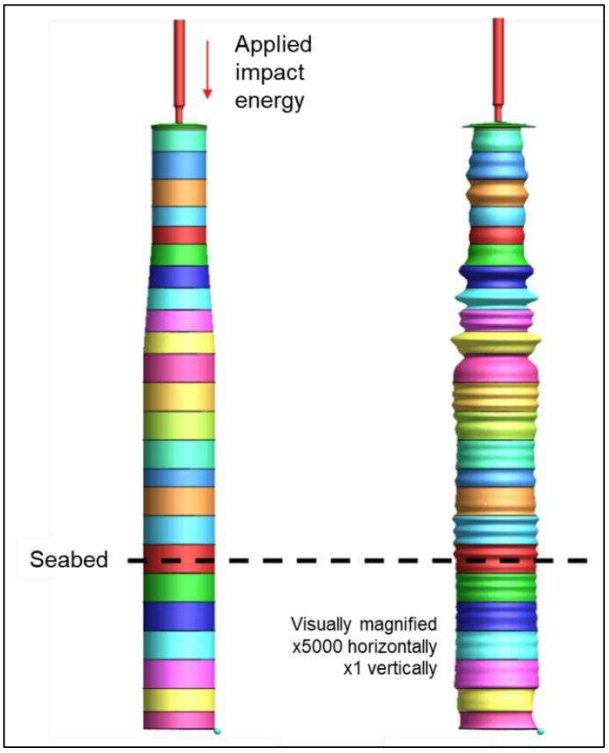

Figure 4. Initial and final position of the MP for the hammer impact analysis, with the radial displacement magnified

2.5 MP-to-boulder push analysis

Due to impact with the MP, the boulder will be displaced thus generating resistance to the MP. Depending upon the impact angle (e.g., direct-hit or glancing blow), the boulder may move vertically downwards or may move laterally and press on the side of the MP during subsequent pile driving. To predict the MP damage during driving, repeated hammer hits could be simulated, however, for computational efficiency, it was preferred to simulate the driving by pushing the MP downwards at a constant rate. A push velocity of 10m/s was chosen for the analysis. The actual MP peak velocity during installation was predicted by GRLWEAP to be lower than this value. However, subject to LS-DYNA sensitivity studies, the 10m/s push velocity was shown to be acceptable. As shown in Figure 6, compared to Figure 1, the adopted model does not include the hammer while a constant velocity is

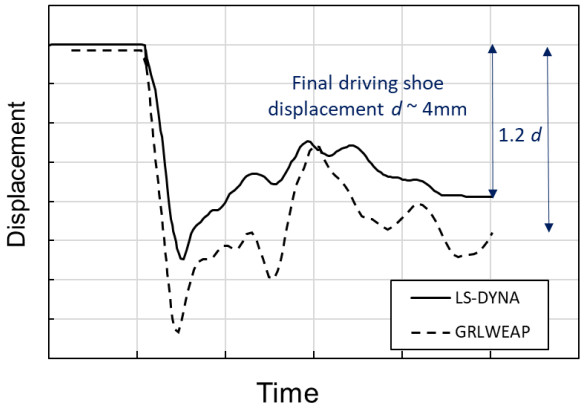

Figure 5. Displacement at the base of MP as predicted by LS-DYNA and GRLWEAP

applied onto the MP . In this type of analysis, it is not necessary to model the full height of the MP, thus only the MP sections which would be below seabed at the final embedment depth are considered. A sensitivity study indicated that, compared to the toe resistance, skin friction does not govern in predicting the plastic strains at the toe of the MP when pushing the MP at a constant velocity (as opposed to hammering the pile). As such, , skin friction was not modelled to keep the model as simple as possible.

2.6 Variables

Four variables were considered in this specific study to explore the effect of: *i)* boulder diameter; *ii)* boulder depth; *iii)* impact angle; and *iv)* soil properties.

The variables of boulder diameter and boulder depth were chosen to reflect the results of the probabilistic boulder assessment study and range of variation for the impact angle during installation. With an impact angle defined as the angle between the horizontal direction and the line between the MP-boulder contact point and the center of the boulder, the variables considered were 45°, 75° and 90°. LB and UB soil profiles were separately evaluated.

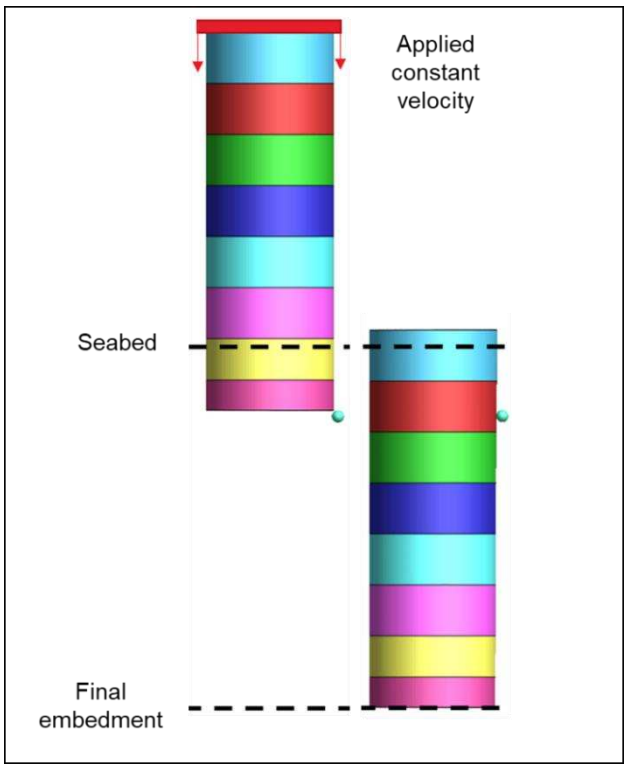

Figure 6. Initial and final position of the MP for the MP-to-boulder push analysis with applied velocity shown

3 RESULTS

3.1 MP-boulder push analysis

Several assessment metrics were used to quantify the damage of the MP due to boulder impact. These included:

1. deformation of the MP;
2. plastic strain and von Mises stress levels in the MP and driving shoe;
3. possible increases in distortion after the impact due to distortional buckling.

Figure 7 shows the deformation at the bottom of the MP at the end of four different MP-to-boulder push analyses. The four analyses consider the variability of the boulder depth and soil properties. In the shown example, the largest MP deformation occurs due to impact with a deep boulder in the UB soil. For this scenario, plastic strains at the driving shoe are shown in Figure 8 for various impact angles (45°, 75° and 90°). The 75° impact angle caused the largest distortion at the bottom of the driving shoe. On the contrary, the 90° impact angle (direct hit) caused the smallest MP distortion with a high localised strain at the contact point between the boulder and MP as the boulder was pushed to the final embedment depth rather than to the side as for the other examined impact angles.

For a particular size and depth of boulder, Figure 9 shows how the MP diameter changes for the UB soil (above) and LB soil (below) during installation. The plotted values of the MP diameter (D) are normalized with respect to its initial diamension (D_0). In this illustrative example, the UB soil causes the MP diameter to continuously reduce, from the time of initial impact to the time of the MP's final embedment. However, in LB soil, the behaviour is different – the MP diameter reaches a plateau after a certain embedment depth. The MP embedded into UB soil will experience greater plastic strains compared to installation of the MP in equivalent LB soil.

By examining the outputs and by comparing the results with maximum admissible limit, design recommendations and installation criteria can be developed.

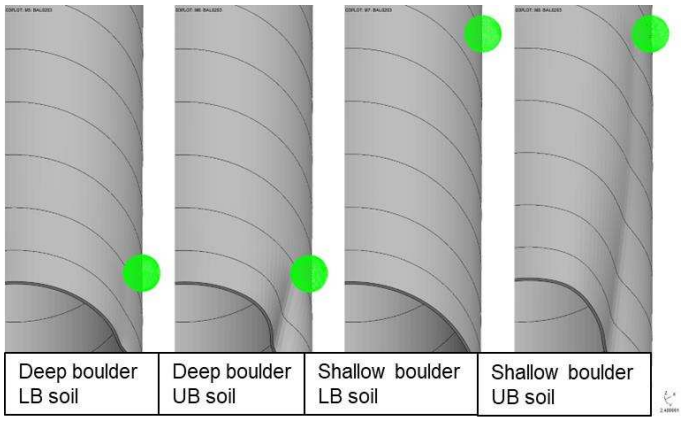

Figure 7. Final deformation of the MP due to boulder impact

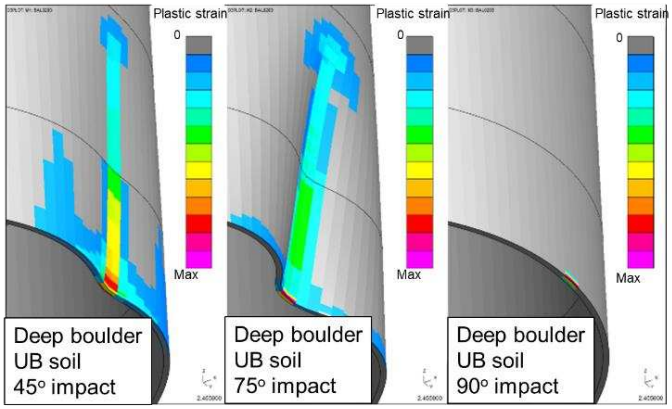

Figure 8. Plastic strains at the driving shoe due to interaction with boulder

3.2 Hammer impact analysis

Figure 10 compares the vertical displacement at the bottom of the MP among three analysis scenarios: *i)* no boulder impact, *ii)* boulder impact angle of 45deg, and *iii)* boulder impact angle of 90deg. It can be seen that displacements are slightly affected by the presence of the boulder if the impact angle is 45deg. In contrast, with an impact angle of 90deg (i.e., boulder vertically moving), the MP displacement reduces compared to the

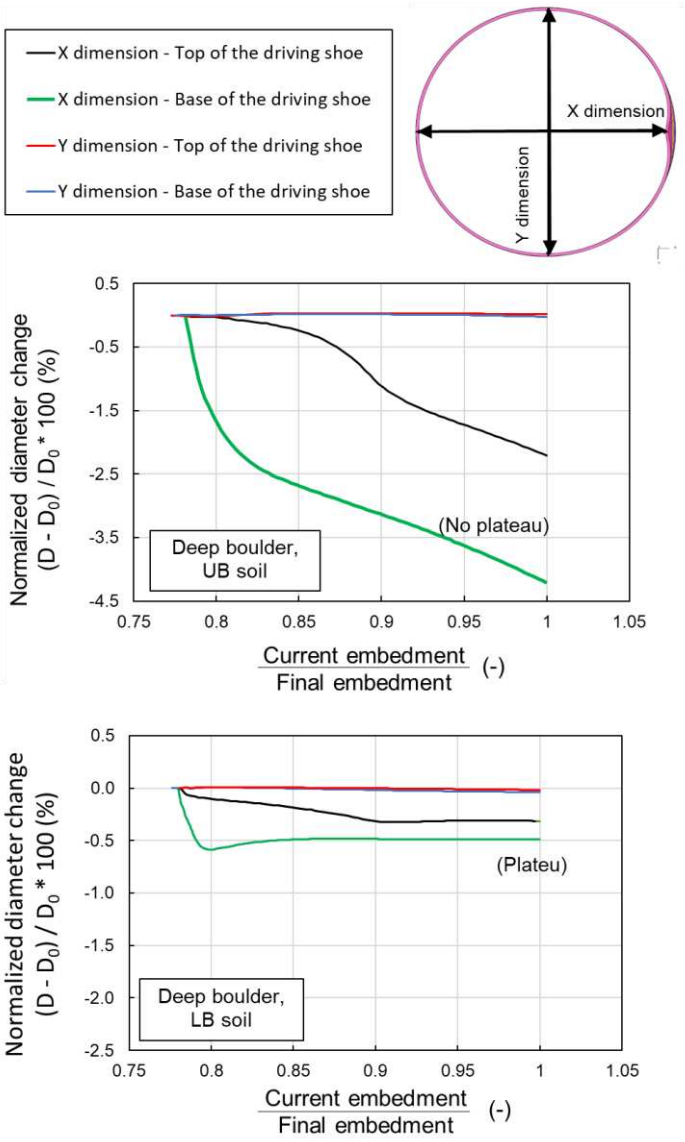

Figure 9. Definition for MP diameter (X and Y) at the base of the MP, and the top of the driving shoe

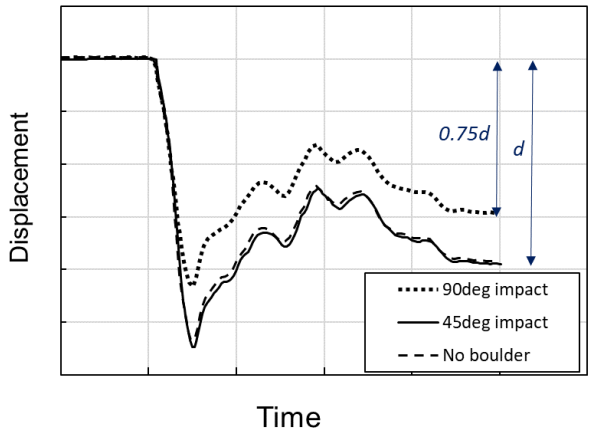

Figure 10. MP toe vertical displacement for three different scenarios

absence of boulder. The observed reduction is due a combination of cross section distortion and pile tilting as a result of the impact.

4 CONCLUSIONS

This paper presents a methodology for managing the risk of installing MPs in sites with embedded boulders which may cause drivability problems, or high stresses that could impact on fatigue curves used for in-service design.

The presented methodology estimates the toe and MP damage due to interaction with boulders during MP installation in offshore applications. In the adopted methodology, the toe and MP damage has been evaluated for both a hammer impact scenario and for a scenario where the MP passes a boulder at constant velocity. In both scenarios, the FE model simplifies the soil surrounding the MP and boulder with non-linear springs and dampers.

The level of damage has been assessed by evaluating the MP distortion and plastic strains at the contact with the boulder and during subsequent driving. A series of variables have been included in the assessment to account for the variability of the site conditions and other uncertainties.

The simplified approach is accessible and practical in terms of processing requirements and turn-around time whilst being capable of making reasonable estimates of MP damage from boulder impacts, along with the effect of such damage on subsequent drivability.

5 REFERENCES

Alm, T. and Hamre, L. 2001. Soil Model for Pile Driveability Predictions Based on CPT Interpretations. *Proceedings of the 15th International Conf. on Soil Mechanics and Foundation Engineering, Istanbul,* Vol. 2, pp. 1297–1302.

Darendeli, M.B., 2001. Development of a new family of normalized modulus reduction and material damping curves. The university of Texas at Austin.

DNV-RP-C208, 2016, *Determination of structural capacity by non-linear finite element analysis methods*, DNV.

Goble, G.G. and Rausche, F. 1976. Wave Equation Analysis of Pile Driving-WEAP Program. Vol. 1-4, FHWA.

Hallquist, J.O., 2006. LS-DYNA theory manual. Livermore software Technology corporation, 3, pp.25-31.

Nietiedt, J., Randolph, M., Doherty, J. and Gaudin, C. 2022. Numerical assessment of tip damage during pile installation in boulder-rich soils. Geotechnique, ahead of print, published online 14 July 2022

Yee, E., Stewart, J.P. and Tokimatsu, K., 2013. Elastic and large-strain nonlinear seismic site response from analysis of vertical array recordings. Journal of Geotechnical and Geoenvironmental Engineering, 139(10), pp.1789-1801.